PERGAMON

Vision Research 41 (2001) 2741–2755

Vision Research

www.elsevier.com/locate/visres

Transducer models of head-centred motion perception

Tom C.A. Freeman *

School of Psychology, Cardiff University, PO Box 901, Cardiff CF10 3YG, UK

Received 21 September 2000; received in revised form 27 April 2001

Abstract

By adding retinal and pursuit eye-movement velocity one can determine the motion of an object with respect to the head. It would seem likely that the visual system carries out a similar computation by summing extra-retinal, eye-velocity signals with retinal motion signals. Perceived head-centred motion may therefore be determined by differences in the way these signals encode speed. For example, if extra-retinal signals provide the lower estimate of speed then moving objects will appear slower when pursued (Aubert–Fleischl phenomenon) and stationary objects will move opposite to an eye movement (Filehne illusion). Most previous work proposes that these illusions exist because retinal signals encode retinal motion accurately while extra-retinal signals under-estimate eye speed. A more general model is presented in which both signals could be in error. Two types of input/output speed relationship are examined. The first uses linear speed transducers and the second non-linear speed transducers, the latter based on power laws. It is shown that studies of the Aubert–Fleischl phenomenon and Filehne illusion reveal the gain ratio or power ratio alone. We also consider general velocity-matching and show that in theory matching functions are limited by gain ratio in the linear case. However, in the non-linear case individual transducer shapes are revealed albeit up to an unknown scaling factor. The experiments show that the Aubert–Fleischl phenomenon and Filehne illusion are adequately described by linear speed transducers with a gain ratio less than one. For some observers, this is also the case in general velocity-matching experiments. For other observers, however, behaviour is non-linear and, according to the transducer model, indicates the existence of expansive non-linearities in speed encoding. This surprising result is discussed in relation to other theories of head-centred motion perception and the possible strategies some observers might adopt when judging stimulus motion during an eye movement.

Keywords: Motion perception; Eye movements; Extra-retinal signals; Filehne illusion; Aubert–Fleischl phenomenon

1. Introduction

Eye movements present an intriguing puzzle to our visual system. In moving the eye we move a largely stationary world across the retina and so sever any straightforward relationship between retinal motion and the motion of objects in the scene. Tracked objects produce no motion on the retina and other objects displace with a retinal velocity that comprises at least two components. One component comes from the projection of the moving object onto the retina and the other from the velocity of the eye movement. For simple movements about the nodal point of the eye, retinal velocity (**R**) is the difference between the object's velocity with respect to the head (**H**) and the pursuit (**P**): $\mathbf{R} = \mathbf{H} - \mathbf{P}$. In more general terms this relationship allows an observer to recover an estimate of the head-centred velocity field ($\hat{\mathbf{H}}$) from current estimates of retinal motion (carried by a retinal signal, $\hat{\mathbf{R}}$) and pursuit velocity (carried by an extra-retinal signal, $\hat{\mathbf{P}}$):

$$\hat{\mathbf{H}} = \hat{\mathbf{R}} + \hat{\mathbf{P}} \tag{1}$$

We refer to this as the transducer model of head-centred motion perception for reasons that will become clearer below. In its various forms the transducer model has been used to explain many phenomena associated with motion perception during eye movements. From a clinical perspective, the transducer model explains the comparative lack of oscillopsia experienced by observers with congenital nystagmus (Leigh, Dell'Osso, Yaniglos, & Thurston, 1988; Bedell & Currie, 1993; Abadi,

* Tel.: +44-29-2087-4554; fax: +44-29-2087-4858.
E-mail address: freemant@cardiff.ac.uk (T.C.A. Freeman).

0042-6989/01/$ - see front matter
PII: S0042-6989(01)00159-6

Whittle, & Worfolk, 1999). The transducer model has also been used to explain why moving objects appear slower when pursued and why stationary objects appear to move against an eye movement (Dichgans & Brandt, 1972; Mack & Herman, 1973; Mack & Herman, 1978; Freeman & Banks, 1998). The model also provides a possible stage in the ability to compute self-motion direction during pursuit (van den Berg, 1992, 1996; Perrone & Stone, 1994; Beintema & van den Berg, 1998; Freeman, 1999; Lappe, Bremmer, & van den Berg, 1999; Freeman, Banks, & Crowell, 2000; Li & Warren, 2000; Royden, Banks, & Crowell, 1992; Royden, Crowell, & Banks, 1994). Given the apparent enthusiasm for the transducer model it is surprising to find that some of its basic properties remain relatively unexplored.

One reason for this may be a preoccupation with the finding that head-centred motion perception alters if certain spatiotemporal characteristics of the retinal image are changed, such as spatial frequency (Dichgans, Wist, Diener, & Brandt, 1975; Wertheim, 1987; Freeman & Banks, 1998), size (Wertheim, 1994), eccentricity and display duration (Mack & Herman, 1978; de Graaf & Wertheim, 1988). Some authors have argued that the change in perceived head-centred motion reflects an extra-retinal signal whose size depends on image characteristics (Raymond, Shapiro, & Rose, 1984; Post & Leibowitz, 1985). Others have argued for a more complex 'reference' signal that combines both retinal and extra-retinal components (Wertheim, 1987, 1994). Both types of argument often ignore the possible errors that arise from retinal signals. In particular, they seem to ignore the many examples in 'eye-stationary' psychophysics showing that perceived speed depends on the spatiotemporal properties of the stimulus (e.g. Smith & Edgar, 1991; Stone & Thompson, 1992; Treue, Snowden, & Andersen, 1993). It would be surprising if these effects did not result from peculiarities intrinsic to retinal motion mechanisms, which in turn implies that any model of head-centred motion perception should incorporate retinal signal errors as well. With this in mind, Freeman and Banks (1998) showed how two classic illusions of head-centred motion perception—the Aubert–Fleischl phenomenon and the Filehne illusion—alter under changes of spatial frequency. More importantly, they showed how the change in these illusions could be predicted from the sum of spatial frequency-dependent retinal errors and an extra-retinal signal whose size depended on pursuit speed alone.

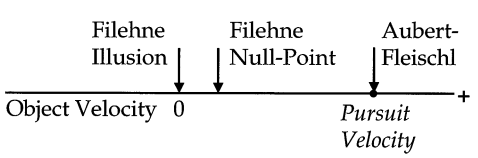

Fig. 1. Object motions studied in head-centred motion experiments are drawn from a range that could be experienced during an eye movement. The transducer model described in the text has principally been investigated by examining two points in this range, the Filehne null-point and Aubert–Fleischl point.

The size of retinal and extra-retinal signals also depends on the relationship between input and output speed. The relationship defines what we shall refer to as a 'speed transducer'. Until recently, the literature on head-centred motion perception has been comparatively silent on the shape of retinal and extra-retinal speed transducers. The principle aim of this paper was therefore to explore transducer shape in detail. Specifically, we investigated the perceptual consequence of combining linear or non-linear transducers and tested the predictions against human perception of head-centred motion.

Previous studies of head-centred motion perception have concentrated on the Aubert–Fleischl phenomenon (Aubert, 1886; Fleischl, 1882) and the Filehne illusion (Filehne, 1922). According to the transducer model, both phenomena imply that extra-retinal signals provide lower estimates of speed than retinal signals. This explains why in the former case a moving object appears to move slower when pursued and why in the latter case stationary objects appear to move in the opposite direction to the eye movement. Of course, if we knew the exact shape of the underlying transducers we could predict the exact size of either illusion for a given pursuit velocity and also how either illusion varies as pursuit velocity changes. However, we do not and so must infer underlying transducer shapes from psychophysical data. The initial theoretical work presented here explores what can be determined from measurements of the Aubert–Fleischl phenomenon and Filehne illusion.

It is important to emphasise that the object velocities used to reveal these two illusions are not the only velocities that an observer might experience when they move their eyes. They are just two points from a range of possible object velocities experienced during an eye movement, as schematised in Fig. 1. The second aim of this paper was therefore to investigate the extent to which transducer models can provide an account of the perception of head-centred velocity anywhere along this continuum.

We have previously proposed that retinal and extra-retinal speed transducers are linear (Freeman & Banks, 1998; Freeman, 1999; Freeman et al., 2000). Turano and Massof (2001) recently carried out a more thorough test of this claim using a general velocity-matching paradigm. In their experiments observers adjusted the direction and speed of a random dot pattern viewed with eyes stationary to match the velocity of the pattern viewed with eyes moving. By stabilising the image (but not the fixation point), Turano and Massof were able to control the retinal motion of the dot pattern indepen-

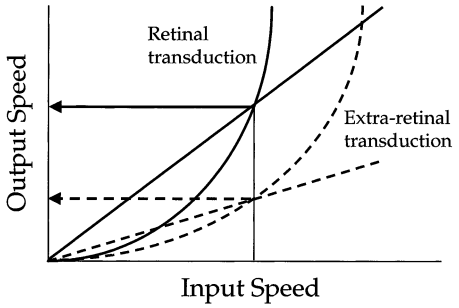

Fig. 2. The idea that extra-retinal, eye-velocity signals yield lower estimates of speed than retinal signals cannot itself reveal the transducer relationship between input and output speed. Any shape of transducer could be used to explain why, for instance, an object moving at a speed defined by the vertical line appears slower when pursued.

dently of any eye movement made. Their rigorous technique produced results that are surprising in many respects. The data obtained for the Aubert–Fleischl phenomenon were well-fit by a straight line. As will be shown below this is characteristic of linear speed transducers. However, the authors chose to compare linear and non-linear models by incorporating these data with those from a general velocity-matching experiment. In the latter, observers were shown dot pattern motion in the pursuit interval sampled from a range similar to that shown in Fig. 1. From model fits to the entire data set they rejected models based on either linear transducers or compressive non-linearities. The model they favoured incorporated a compressive retinal signal and a composite 'compensating signal' comprising both retinal and extra-retinal components. As they noted, this is similar to Wertheim's (1994) reference-signal model. The claim is that perceived head-centred motion is not simply the sum of retinal and extra-retinal signals (as in Eq. (1)) but a function of retinal and reference signals, the latter comprising retinal and extra-retinal components.

Turano and Massof's study raises many interesting questions, some of which we investigated here. For instance, while the reference-signal model accounts for their whole data set, one must ask why their data for Aubert–Fleischl phenomenon could also be adequately accounted for by linear transducers. In general velocity matching, observers are asked to pursue one target while judging the velocity of another. This is an unusual fixation strategy for judging the velocity of a moving object and so this may be the reason why the observed matching behaviour is not easily accounted for within the transducer framework. Alternatively, as one of the reviewers pointed out, non-linear behaviour could be less pronounced in this condition because the retinal speed experienced by their observers during pursuit was less. In Turano & Massof's Aubert–Fleischl condition, the 'pursued' retinal speed was 0 (by definition) whereas in the other two conditions they investigated it was 2°/s and 4°/s, respectively. Their model fit the data of all three conditions well, indicating that the non-linearities defined in their model have a greater impact at higher 'pursued' retinal speeds. However, the range of pursuit speeds was the same regardless of condition and the test retinal speed in the eye-stationary interval (as set by the observer) did not vary that much between conditions. Moreover, test and standard retinal motions covered approximately the same speed range over all conditions studied. As all three types of motion must undergo some form of speed transduction, it is unclear to us in which condition one might expect significant markers of non-linear behaviour.[1]

One can also ask whether inferences drawn from an image stabilisation technique generalise to normal viewing given that this is not a typical viewing situation. It is also not obvious from Turano & Massof's data what is the best account for the Filehne illusion. Lastly, the range of retinal and extra-retinal speeds examined was relatively low in the context of work on head-centred motion perception.

To explore these and other issues we begin by examining linear and non-linear transducer models of the Aubert–Fleischl phenomenon. There are two reasons for this. The first is that the method used to measure the size of this illusion involves speed matching between eye-stationary and eye-pursuit intervals whereas all other points in the range depicted by Fig. 1 call for both speed and direction to be matched by the observer. The second reason is that non-linear transducer models of the type examined here are intractable for all points other than the Aubert–Fleischl and so their behaviour is less transparent.

2. Modelling the Aubert–Fleischl phenomenon

A moving object typically appears slower when pursued (though see Freeman & Banks (1998) and Dichgans et al. (1975) for exceptions to this rule). To establish this an observer must compare two conditions. In one they track the object with an eye movement (we shall assume that the eye movement is accurate) while in the other they view the object with stationary fixation. According to the transducer model, perceived motion is mediated by extra-retinal signals in the eye-pursuit condition and retinal signals in the eye-stationary condition (e.g. Dichgans & Brandt, 1972). Extra-retinal signals therefore produce the lower estimate of speed. As Fig. 2 demonstrates, however, any

[1] Also relevant is our finding that the Filehne illusion is best accounted for by the linear model, despite the fact that this condition contains non-zero 'pursued' retinal motion.

transducer shape can be made to produce the same magnitude of slow-down for a given object speed. To discriminate between various transducer shapes a range of object motions must be investigated so that a range of pursuit and retinal speeds are examined.

The predictions of a linear transducer model are straightforward. The linear transducers are completely described by two parameters, e and r, which we term the extra-retinal and retinal gains, respectively. The gains represent the slope of the linear relationship between speed input and speed output (e.g. pursuit speed and extra-retinal signal). In the speed-matching experiment, an observer views two intervals: an eye-pursuit interval in which the object and eye move at a speed P and an eye-stationary interval in which the object moves at speed H. We use the symbol H to emphasise the point that retinal and head-centred speed (and velocity) are the same when the eye is not moving and the head is still. The task for the observer is to produce a perceived-speed match between the two intervals by adjusting the eye-stationary speed until it matches the head-centred speed in the pursuit interval. In our experiments, a staircase method was used to control the adjustment.

When then speeds of the two intervals match:

$$H = \frac{e}{r} P \tag{2}$$

The implication, often overlooked, is that individual gains cannot be determined (even if you try and measure r by keeping the eye stationary: see Freeman & Banks, 1998, for a more detailed discussion). Put another way, the Aubert–Fleischl phenomenon could be the result of under-estimating eye speed in the pursuit interval; but equally so, it could be the result of over-estimating the speed of retinal motion in the eye-stationary interval. In fact, the possibilities are limitless.

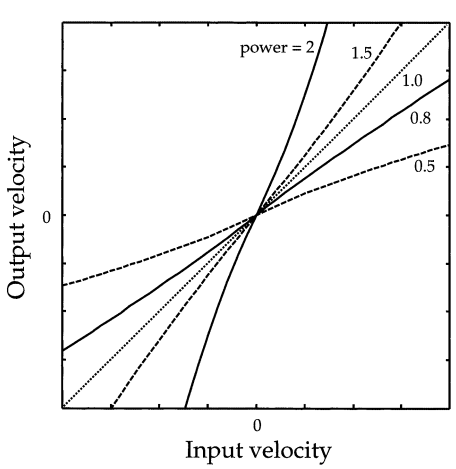

Fig. 3. Examples of non-linear speed transducers produced by the augmented power-law function of Eq. (3) with $a = 1$. An important property is that the family of functions cross at the origin and nowhere else.

The predictions for a non-linear transducer model depend on the type of non-linearity assumed. Theoretical and empirical studies of retinal motion perception have largely ignored mechanisms for recovering speed (let alone the shape of speed transducers) and so there is little guidance on a suitable candidate. Turano and Massof (2001) assumed that transducers were either linear or compressive (i.e. saturating); we relax that constraint and allow expansive transduction for reasons that will become more evident later. To do this we based our transducer on an augmented power-law:

$$\mathbf{V}_{\text{out}} = \text{sgn}(\mathbf{V}_{\text{in}}) \times [(|\mathbf{V}_{\text{in}}| + a)^p - a^p] \tag{3}$$

where $\text{sgn}(\mathbf{V}_{\text{in}})$ is the signum function and gives direction, taking on values of $+1$ for rightward movement and -1 for leftward. Generalising to other directions is possible but beyond the scope of the present paper. $|\mathbf{V}_{\text{in}}|$ is the input speed. The parameter a was fixed to 1 throughout. Fig. 3 provides examples of this function for a range of exponents.

With $a = 0$ one obtains a more straightforward power law. However, this simpler form produced worse fits to the data than the family of transducers shown in Fig. 3. One reason for this is that when $a = 0$, transducers with different exponents are now forced to cross at (1, 1). Consequently, for a pursuit speed of 1°/s no Aubert–Fleischl phenomenon or Filehne illusion is predicted. Our results, however, show that they exist. Another consequence is that the simpler form predicts a reversal of both illusions below pursuits of 1°/s, although we hasten to point out that these low pursuit speeds were not examined in our experiments.

At the match point, the non-linear model predicts:

$$\log(H + 1) = \frac{\varepsilon}{\rho} \log(P + 1) \tag{4}$$

where ε and ρ correspond to the extra-retinal and retinal exponents of the two non-linear transducers, respectively. As with the linear model, the individual parameters cannot be determined. Both linear and non-linear models of the Aubert–Fleischl phenomenon therefore have one free parameter, corresponding to the gain or power ratio, respectively.

It is also possible to combine linear and non-linear transducers to produce a speed function consisting of Eq. (3) multiplied by a gain term. We refer to this as a hybrid transducer. Combining two hybrid transducers always produced superior fits to the data compared to either of the transducers described above, which is hardly surprising as the hybrid model contains at least twice the number of free parameters. However, the superiority was negligible.

In Experiment 1, we sought evidence to distinguish between linear and non-linear models by investigating the Aubert–Fleischl phenomenon over a wide range of object speeds.

3. Experiment 1

3.1. Stimuli

Moving objects were depicted using sparse random dot patterns (density ≈ 0.64 dots/deg^2) displayed on the dark background of a Mitsubishi Diamond Pro 20 monitor. The monitor was driven by a VSG2/3F graphics card under PC control. The random dot pattern moved horizontally across the screen. This was achieved by simulating an eye rotation about the vertical axis using standard projection techniques. On each frame, dot position was rendered with sub-pixel accuracy by controlling the centroid of a 2×2 pixel cluster using an anti-aliasing technique. From the viewing distance of 57.3 cm the cluster subtended approximately 0.08°. The luminance of the display was gamma-corrected.

Random dot patterns were displayed through a software-generated annulus window (inner radius = 1°, outer radius = 5°). The window moved with the same velocity as the fixation point. The fixation point consisted of a short, vertical line that appeared 400 ms before and after the random pattern. The dot pattern itself was displayed for 700 ms.

In all experiments, observers were instructed to judge motion with respect to the head. To encourage this, experiments were conducted in the dark so that no incidental visual references were visible to the observer. No observer reported they could see anything (including the edge of the screen) other than dot pattern and fixation point. To control for possible influences of motion after-effects, the direction of motion alternated from trial to trial in Experiments 1 and 2 and from setting to setting in Experiment 3. Viewing was always monocular and the observer's head was supported by a chin-rest.

3.2. Eye movement recording and analysis

Eye movements were recorded using a head-mounted video-based eye-tracker (ASL Series 4000). Recording sessions were carried out using software and calibration routines supplied by ASL. Eye position was recorded at a sampling rate of 50 Hz and eye velocity determined using customized software written in MatLab. The time derivative was taken for low-pass filtered eye position recordings and then saccades detected using a velocity criterion of ± 40°/s. As Leigh and Zee (1999) note, the value used for the velocity threshold is somewhat arbitrary. They suggest a value of 30°/s. Velocity thresholds around this value are able to detect saccades around 1° in amplitude (Bahill, Iandolo, & Todd Troost, 1980; Yee, Daniels, Jones, Baloh, & Honrubia, 1983).

Any records found containing saccades were removed from subsequent analysis. Inspection of individual records confirmed that the recordings deemed saccadic were being detected correctly. Mean eye-velocity for any particular trial was then computed by averaging over samples in which the dots patterns were visible, typically the central 700 ms of any stimulus interval.

3.3. Observers

The author (TCAF) and three other observers participated in the experiments. None of the observers knew the hypotheses of the experiments apart from the author. CHT was an inexperienced psychophysical observer and was paid for her participation; JJN had some previous experience and JHS was an experienced psychophysical observer.

3.4. Procedure

Speed matches for the Aubert–Fleischl phenomenon were obtained using a two-interval, forced-choice technique. In the first pursuit interval the random dot pattern, fixation point and annulus window moved at a speed of 1, 2, 4, 8 or 16°/s. In the second eye-stationary interval only the random dot pattern moved. Observers indicated which of the two intervals appeared to move faster with respect to the head. A 1-up 1-down staircase controlled the speed in the second interval. Step sizes were adjusted logarithmically. Speed matches were determined by taking the geometric mean over the final 8 reversals. Each experimental session investigated one pursuit-interval speed, using two randomly interleaved staircases. Observers carried out at least one session before any data were collected.

3.5. Results and conclusions

Settings were similar for all four observers and so Fig. 4 plots the mean eye-stationary speed match as a function of pursuit-interval object speed. The thin oblique line plots the expected speed match if no illusion were suffered. All data fall below this, indicating that observers exhibited a classic Aubert–Fleischl phenomenon at all object speeds.

Both linear (solid line) and non-linear (dashed line) models were fit to the data using a least-squares minimisation technique implemented in MatLab. The best-fitting gain and power ratios are shown in the Figure, along with a measure of the goodness-of-fit known as the coefficient of variation (R^2). This measure, which is equal to $1 -$ residual sum-of-squares/total sum-of-squares, quantifies the error between model and data scaled by the total variability in the data: a value of 1 indicates a perfect fit and a value of 0 indicates a very poor fit (note that R^2 can go negative in exceptional circumstances if the variability of the residuals is

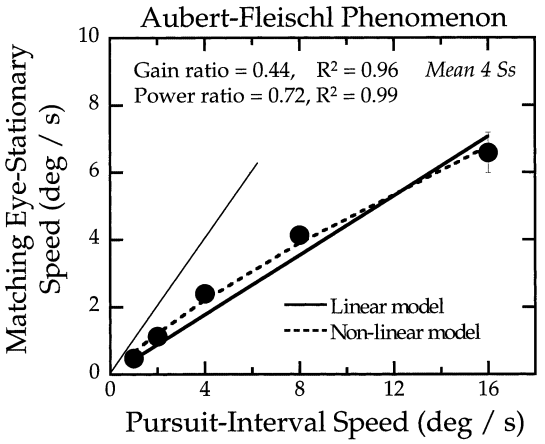

Fig. 4. The Aubert–Fleischl phenomenon as a function of pursuit-interval speed. The data points are the mean of four observers. The thin oblique line defines veridical speed matching (i.e. no Aubert–Fleischl phenomenon). The solid and dashed lines show the best-fitting linear and non-linear models, respectively. The best-fitting gain and power ratios, together with the corresponding goodness-of-fit measure (R^2), are given in the inset. Error bars are ± 1 S.E. and are typically smaller than the symbol size.

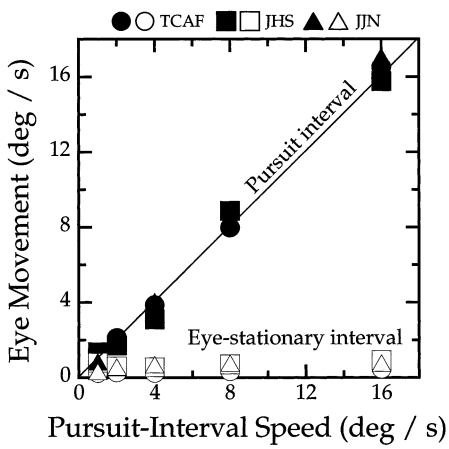

Fig. 5. Eye movements made for three of the observers who contributed data to Fig. 4. Solid symbols correspond to eye movements made in the pursuit interval movements and open symbols to those made in the eye-stationary interval. The thin oblique line defines perfect pursuit for the pursuit interval. Error bars are ± 1 S.E. and are smaller than the symbol size.

greater than the variability of the data). Another interpretation of R^2 is that it defines the proportion of variance in the data explained by the model (Fotheringham & Knudsen, 1987).

The values of R^2 are high in both cases, with the non-linear model producing a value closer to one. The best-fitting power ratio and gain ratio were less than one, indicating that the extra-retinal transducer rises more slowly than its retinal counterpart. To reiterate, however, we cannot tell whether the underlying transducers under or over-estimate input speed in the case of linear mechanisms, or compress or expand input speed in the case of non-linear mechanisms. The hybrid model (in which both gain and power are free to vary) produced a negligible improvement to the fit ($R^2 = 0.995$). It is also clear from the non-linear fit that little improvement would be obtained if the parameter a in Eq. (3) were allowed to vary as well. Our data are in agreement with that of Turano and Massof (2001) over the smaller range of speeds they studied. From their Fig. 3, the maximum pursuit ranged from approximately 3 to 4°/s depending on observer. The maximum retinal speed varied over about the same range (again depending on observer). Over this reduced range a linear model would fit our data well (though note there are only three points). Over the total range of speeds investigated here, the non-linear model provides the superior fit. However, the departure from linearity is small given the 16-fold change in object speed.

Fig. 5 summarises eye movements made by three of the four observers. The pursuit interval data are plotted as closed symbols; the diagonal line defines accurate pursuit. The eye-stationary data are plotted as open symbols. All three observers were able to track the fixation point reasonably accurately in the pursuit interval, though JHS was more variable than TCAF and JJN. Small optokinetic movements were evident in the in the eye-stationary interval, though on average these were negligible as shown by the figure. The best-fitting models of Fig. 4 assume accurate eye movements and there is little reason to suppose this is not the case. Accurate pursuit is to be expected because the fixation movement was predictable and, unlike the next two experiments, the only object visible during pursuit moved at the same velocity as the fixation point.

4. Modelling the Filehne illusion

A stationary object typically appears to move in the opposite direction to an eye movement (though see Wertheim, 1987, Haarmeier & Thier, 1996 and Freeman & Banks, 1998 for exceptions to this rule). Referred to as the Filehne illusion, this finding is another example of the mismatch between retinal and extra-retinal signals. One method for measuring the size of the illusion is to allow the object to move and have observers adjust its head-centred (i.e. screen) velocity **H** until the object appears stationary. Observers must therefore take into account both the speed and direction of eye movement and retinal motion.

At the null-point, retinal and extra-retinal signals are equal and opposite (i.e. $\hat{\mathbf{R}} = -\hat{\mathbf{P}}$). Under this assumption, the linear model predicts:

$$\mathbf{H} = \left(1 - \frac{e}{r}\right)\mathbf{P} \tag{5}$$

The null velocity **H** should therefore be a linear function of pursuit speed **P** with a slope of one minus the gain ratio. The results of Experiment 1 suggest that the actual slope should be small and positive if the same mismatch applies to the Aubert–Fleischl phenomenon and Filehne illusion.

The non-linear model is complicated by the fact that we must consider both speed and direction. Applying Eq. (3) with $a = 1$ to the retinal and pursuit speeds at the null-point:

$$\mathrm{sgn}(\mathbf{H}-\mathbf{P}) \times [(|\mathbf{H}-\mathbf{P}|+1)^{\rho}-1] = -\mathrm{sgn}(\mathbf{P}) \times [(|\mathbf{P}|+1)^{\varepsilon}-1] \quad (6)$$

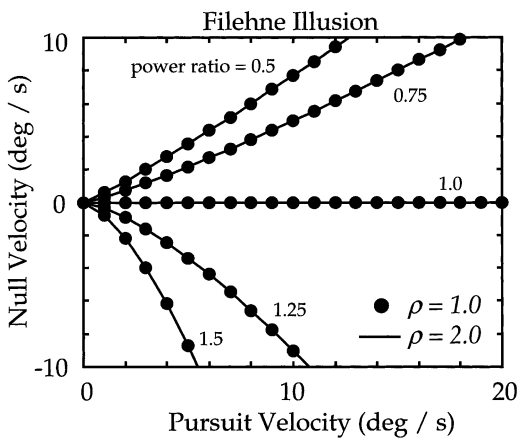

Fig. 6. Computer simulations of the Filehne illusion using non-linear speed transducers. Each function describes the predicted null velocity as a function of pursuit velocity for a number of different power ratios. Positive null velocities are in the same direction as the pursuit. The lines are based on a retinal power of 1 and an extra-retinal power producing the power ratio indicated. The symbols correspond to a doubling of both powers. Like the Aubert–Fleischl phenomenon, null velocity is determined by power ratio only.

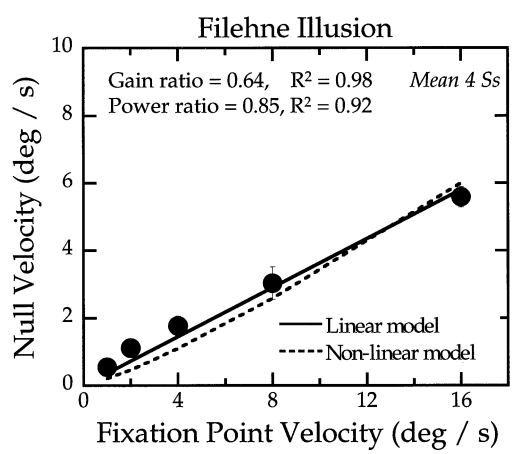

Fig. 7. The Filehne illusion as a function of fixation-point velocity. The data points are the mean of four observers. The solid and dashed lines show the best-fitting linear and non-linear models, respectively. The best-fitting gain and power ratios, together with the corresponding goodness-of-fit measure (R^2), are given in the inset. Error bars are ± 1 S.E.

The left-hand side of this equation represents the non-linear retinal signal (because $\mathbf{H}-\mathbf{P}$ is the retinal velocity) and the right-hand side the equal and opposite extra-retinal signal. Eq. (6) is intractable; one cannot solve for **H**. Predictions for the non-linear model of the Filehne illusion were therefore investigated by computer simulation. For a given pursuit velocity and pair of retinal and extra-retinal powers (ε and ρ), the retinal velocity ($\mathbf{H}-\mathbf{P}$) was adjusted by altering head-centred velocity (**H**) until retinal and extra-retinal signals satisfied the equality represented in Eq. (6). The adjustment was controlled by least-squares minimisation using MatLab's simplex search algorithm.

The principle question is whether the Filehne null-point is dependent on the power ratio. Fig. 6 demonstrates this to be the case. The lines in Fig. 6 correspond to simulations using a retinal power $\rho = 1$ with extra-retinal powers (ε) that yielded power ratios of $\varepsilon/\rho = 0.5$ (top line) up to $\varepsilon/\rho = 1.5$ (bottom line). The symbols depict a second simulation in which both powers were doubled, thereby keeping the power ratio the same. In each case symbols plot on top of lines. The simulations therefore demonstrate that as with the Aubert–Fleischl phenomenon, nulling the Filehne illusion can only reveal the ratio between powers of underlying (non-linear) transducers.

5. Experiment 2

5.1. Procedure

The random dot stimuli were identical to those used in Experiment 1. The Filehne null-point was determined using a single-interval forced-choice procedure. Following each trial, the observer indicated whether the stimulus appeared to move leftward or rightward with respect to the head. The velocity of the stimulus was controlled by a 1- up 1-down staircase that adjusted speed in linear steps. The direction of motion was alternated from trial to trial. Each session comprised two randomly interleaved staircases and pursuit speeds of 1, 2, 4, 8 or 16°/s. Null velocities were based on the arithmetic means over the last eight reversals of each staircase. As in Experiment 1, the display duration was 700 ms.

5.2. Results and conclusions

Settings were similar across the four observers and so Fig. 7 plots mean null velocity against pursuit velocity. The data lie above a null velocity of 0. This implies that each observer suffered a classic Filehne illusion: they had to move the dot stimuli in the same direction as the pursuit in order to null the illusory motion.

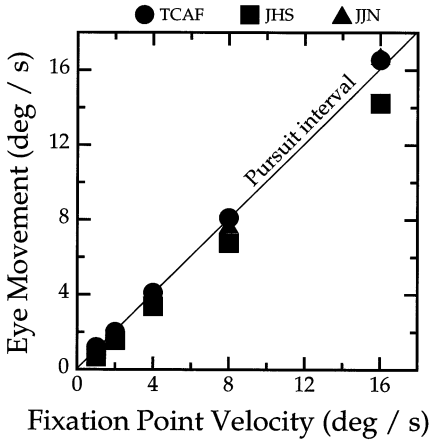

Fig. 8. Eye movements made by three of the observers contributing to the data of Fig. 7. The oblique line corresponds to perfect pursuit. Error bars are ± 1 S.E.

The non-linear model was fit to the data using a least-squares technique based on that used to generate Fig. 6. Note that this necessarily involves two concurrent minimisation routines: for any candidate power ratio, the first solves for **H** given the intractable nature of Eq. (6); the second then adjusts the power ratio until the best least-squares fit between model and data is obtained. The linear model (solid line) gives a better account of the data than the non-linear model (dashed line) but again, as with the Aubert–Fleischl phenomenon, the difference in fit between the models is not large. The hybrid model produced a small improvement to the fit. In each case accurate pursuit was assumed. Unlike Experiment 1 this is a questionable assumption because for most of Experiment 2 observers were attempting eye pursuit over a background moving differently from the pursuit target. In this situation pursuit gain is known to decrease (Yee et al., 1983; Collewijn & Tamminga, 1984). Fig. 8 plots the eye movements made for three of the four observers. If there is any significant lowering of pursuit gain then it occurs for observer JHS alone (note in most cases the symbols for TCAF and JJN plot on top of each other). To investigate the impact of inaccurate eye movements on our conclusions we therefore used the pursuit gains of JHS to alter **P** in Eq. (6) and then refit the model to the mean data of Fig. 7. The effect on best-fitting parameter value and R^2 was negligible (linear model: gain ratio = 0.59, $R^2 = 0.97$; non-linear model: power ratio = 0.81, $R^2 = 0.89$).

Within the context of Experiments 1 and 2 we find little reason to reject the linear model. The reason we draw this conclusion is not just because the linear model provides the better account of the data in Experiment 2, nor that the departures from non-linearity are small given the 16-fold change in pursuit speed in Experiment 1. It is because there is little difference to be had between linear and non-linear accounts of these two illusions, in which case the deciding principle is one of parsimony.

6. Modelling general velocity matching

As discussed earlier, the matched Aubert–Fleischl phenomenon and nulled Filehne illusion are two points from a range of possible head-centred object velocities experienced during an eye movement (Fig. 1). Turano and Massof (2001) have studied this range in some detail and concluded that neither linear or 'simple' non-linear accounts like those examined above could account for the data. As pointed out in the Introduction, their technique relied on image stabilisation which leaves open the question of what happens during everyday unstabilised viewing. It is also unclear whether the theoretical ambiguity over transducer shape (i.e. that matches are determined by gain or power ratio only) applies to general velocity matching as well.

In general velocity-matching, the task for the observer is to adjust the velocity of an eye-stationary interval ($\mathbf{H}_{es}$) to match that of a pursuit interval consisting of both pursuit (**P**) and a dot pattern moving at a head-centred velocity ($\mathbf{H}_{p}$). The latter is drawn from the range shown in Fig. 1. According to the linear model (see Appendix A for derivation), the two intervals appear to match when:

$$\mathbf{H}_{es} = \mathbf{H}_{p} + \left(\frac{e}{r} - 1\right)\mathbf{P} \tag{7}$$

Matched velocity therefore increases with a slope of one when plotted against the head-centred velocity in the pursuit interval, and has a y-axis intercept dependent on pursuit velocity and gain ratio. According to the results of the first two experiments, we expect general velocity-matching data to produce a straight-line graph with a negative intercept. Like the Aubert–Fleischl phenomenon and Filehne illusion, general velocity matching reveals gain ratios only.

The non-linear transducer model is intractable. At the match point, one obtains a cumbersome equation with three components (see Appendix A). On the left-hand size is the transduced retinal velocity of the eye-stationary interval; on the right-hand side is transduced retinal velocity accompanying the pursuit interval, plus the transduced pursuit velocity. Computer simulation was therefore used to determine the predictions of the non-linear model. The simulation technique was similar to that described for the Filehne illusion.

Fig. 9 plots matching functions for various combinations of retinal and extra-retinal powers. The most intriguing aspect of the non-linear model is that the matching functions are unique to the absolute value of the powers used, apart from two points where all functions cross. In Fig. 9A, each curve is based on

individual retinal and extra-retinal powers that all yield a ratio of 1. As one moves from the upper functions to the lower functions the underlying transducers change from expansive squares to compressive square-roots. The two points at which the functions cross correspond to the nulled Filehne on the left and the matched Aubert–Fleischl on the right. At these points, one cannot discriminate between the individual powers; only power ratio can be determined as shown earlier. For comparison, a similar set of predictions has been generated in Fig. 9B for a power ratio of 0.8 (close to the best-fitting power ratio of Experiments 1 and 2). Again, the matching functions are unique to the individual powers used and they cross at two points corresponding to the Aubert–Fleischl phenomenon and Filehne null.

Why do we find these unique predictions away from the Filehne null-point and Aubert–Fleischl match-point? It is obviously difficult to intuit the properties of the non-linear model; one pointer is that for velocities other than those corresponding to the two illusions, the equation at the match point consists of two retinal terms and one extra-retinal term. However, the second retinal term disappears at the point where the matching functions cross.

On the basis of Fig. 9 it would appear that the actual shapes of individual transducers could potentially be determined. This is only partially true: one can recover the individual shapes but only up to an arbitrary scaling factor. To demonstrate this, the symbols in Fig. 9A plot the predictions of the hybrid model for the same combinations of retinal and extra-retinal powers used to determine the lines but with retinal and extra-retinal scale factors set to 0.5 (note that the non-linear model is simply a particular instance of the hybrid model with scale factors set to 1). Symbols and lines plot on top of each other and hence shape can be determined up to an unknown scale. Nevertheless, Fig. 9 demonstrates that one is able to distinguish between compressive and expansive transducers which is not the case for the Aubert–Fleischl phenomenon or Filehne illusion. It appears that the least-informative points to study are those that have received the most attention in the literature!

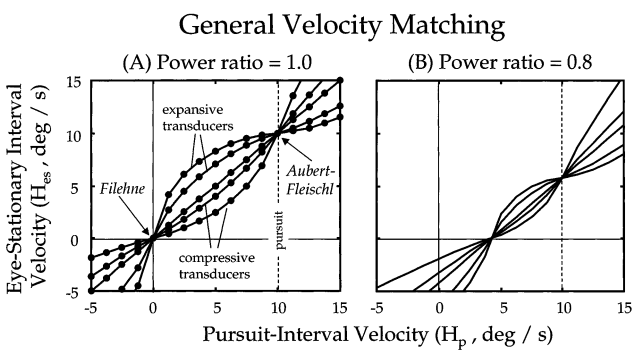

Fig. 9. Computer simulations of general velocity matching using non-linear transducers. The left panel shows simulations for a power ratio of 1. The five matching functions were produced using powers $\rho = \varepsilon = 2$ (top curve), 1.5, 1, 0.8 and 0.5 (bottom curve). The right panel shows simulations based on the same retinal powers but extra-retinal powers changed to produce a power ratio of 0.8. The symbols in the left panel correspond to simulations using hybrid transducers, in which the non-linear transducers were scaled by a factor of 2. See text for details.

7. Experiment 3

7.1. Procedure

Stimuli identical to those described above were incorporated into the following method-of-adjustment procedure. Each trial comprised a pursuit interval and an eye-stationary interval shown in sequence. The task for the observer was to adjust dot velocity in the eye-stationary interval until the perceived head-centred velocities of the two intervals matched. The pursuit interval consisted of a fixation point and window moving at one of three speeds ($\mathbf{P} = 2.5$, 5 and 10°/s) and a dot pattern moving at a head-centred velocity ($\mathbf{H}_p$) drawn at random from the range -5 to $\mathbf{P} + 5$°/s. The eye-stationary interval consisted of a stationary fixation point and window, and a dot pattern moving at a velocity ($\mathbf{H}_{es}$) that could be adjusted by the observer. The dot velocity of the eye-stationary interval was initially chosen at random. Following each trial, observers adjusted the eye-stationary dot velocity using one of six speed increments/decrements that ranged from 0.25°/s to 8°/s in octave steps. The trial was then repeated at the new eye-stationary velocity and the observers made another adjustment if necessary. Observers continued in this fashion until satisfied with their setting, at which point a new head-centred velocity was selected for the pursuit interval and the procedure repeated.

Pursuit direction was alternated between settings not between trials. Each experimental session examined one pursuit speed only and consisted of 30 randomly-selected velocities. Each observer carried out at least three sessions. The results are based on the final two sessions.

7.2. Results and conclusions

Fig. 10 shows the settings made by four observers for a pursuit speed of 10°/s. The vertical axis plots the eye-stationary velocity setting and the horizontal axis the head-centred velocity of the dot pattern that accompanied the pursuit. We emphasise that each panel contains 60 raw data points and so gives a rather direct indication of individual variability. The variability was less at lower pursuit speeds as one might expect. Solid lines correspond to the best-fitting linear model; broken

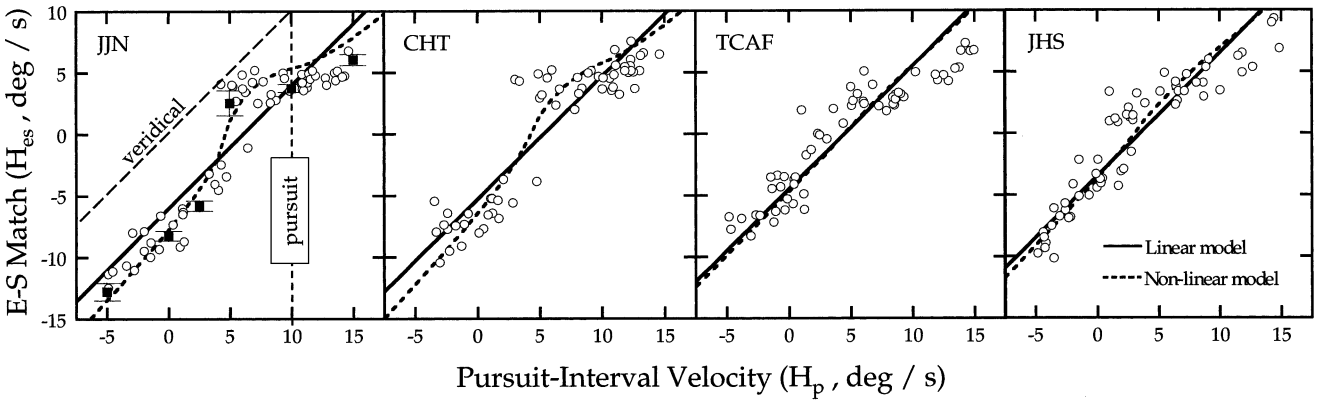

Fig. 10. General matching functions for four observers. Each panel corresponds to a different individual. The pursuit speed was 10°/s; positive velocities correspond to random dot patterns that moved in the same direction as the fixation point. Each panel contains 60 raw data points. The solid squares in the left panel show a replication of the experiment for observer JJN using a staircase method; the error bars in this case represent ± 1 S.E. The best-fitting linear and non-linear models are shown using solid and dotted lines, respectively. The dashed oblique line in the left panel defines veridical velocity matching.

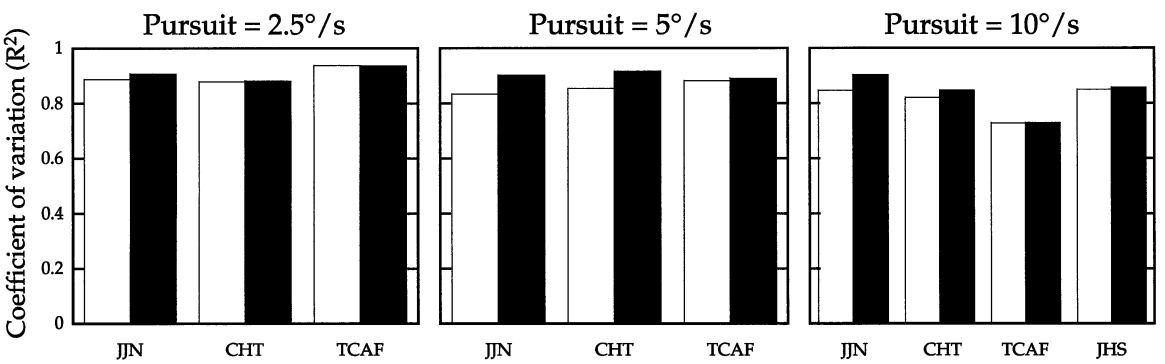

Fig. 11. Goodness-of-fit as a function of observer for each of the three pursuit speeds studied. Note that observers JHS participated in the 10°/s condition only.

lines to the best-fitting non-linear model, fit using a technique similar to that described for the Filehne illusion. For JJN, CHT and TCAF, the models were fit across all three pursuit speeds simultaneously. JHS only participated in the 10°/s condition and so the fits for her are based on that pursuit speed alone. The hybrid model was also fit to each observer's data but produced identical fits to the non-linear model.

Fig. 11 compares the goodness-of-fit of both models by plotting the R^2 values at each pursuit speed. Solid bars correspond to the non-linear model. The results indicate some variability across observers. For JHS and TCAF there is little to choose between the two models. For JJN and CHT the non-linear model produces the better fit for pursuit speeds of 5 and 10°/s. The best-fitting power ratio ranged from 0.77 to 0.86 and the best-fitting gain ratio ranged from 0.39 to 0.65. These values are similar to those found in Experiments 1 and 2.

The surprising finding is that when the matching functions depart markedly from linearity (e.g. JJN and CHT in Fig. 10), expansive non-linearities were required to improve the fit. Fig. 12 shows the best-fitting retinal and extra-retinal powers for each observer. In almost all cases the powers are 1 or above.

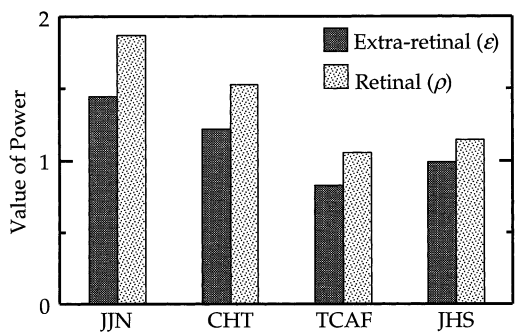

Fig. 12. Best-fitting powers for non-linear retinal transducers (light bars) and extra-retinal transducers (dark bars).

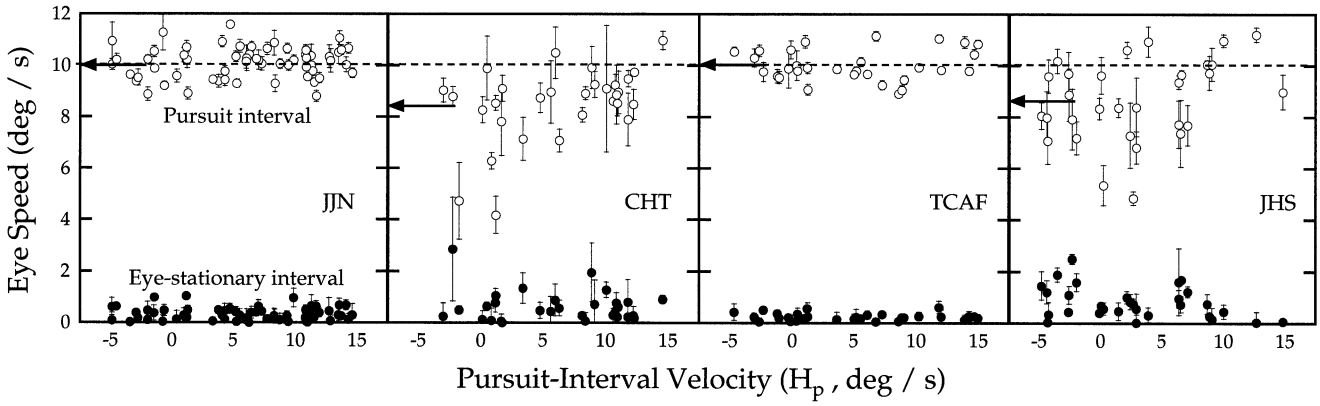

Fig. 13. Eye movements during general velocity matching. Open symbols correspond the pursuit-interval stimuli and closed symbols the eye-stationary intervals. Arrows indicate the mean pursuit collapsed over pursuit-interval velocity. Error bars are ± 1 S.E.

The expansive behaviour is not peculiar to the method-of-adjustment. The solid squares in the left panel of Fig. 10 plot the velocity matches found for observer JJN using a 1-up 1-down staircase technique. The data from the two techniques are in close agreement. Experiment 3 was also repeated on the three main observers using a shorter display duration of 300 ms. The results (not shown) were similar to those shown in Fig. 10.

The model fits assume that the eye movements were accurate but a possible explanation for the apparently non-linear behaviour is that eye movements depended on dot velocity in the pursuit interval. Fig. 13 plots the result of the eye movement analysis for a pursuit of 10°/s. For observer JJN, eye movements were recorded during both sessions. For the remaining observers, eye movements were recorded in one of the two experimental sessions. The data show that eyes remained approximately still in the eye-stationary interval (closed symbols). In the pursuit interval (open symbols) there is no suggestion of a marked relationship between actual pursuit speed and velocity in the pursuit interval. Although there appears to be considerable variability in the eye movements made, it must be emphasised that each data point is a mean based on a handful of recordings only. On average observers made around 5 reviews per condition and some of the recordings were rejected because saccades were detected. A better indication of performance is given by the mean eye movement for each observer collapsed across condition. These are shown as arrows in the Figure. The mean pursuit gain across observers was 0.93 which is reasonably accurate and compares favourably to previous reports (e.g. Meyer, Lasker, & Robinson, 1985). Both this and the lack of relationship between accuracy and dot-pattern velocity explains why, when the model was refit using these data, little change in fit was found for two observers (TCAF & JHS) whereas the effect for CHT and JJN was to make the inferred transducers more, not less, expansive.

The final point to consider is the lack of eye-stationary settings of 0 in JJN's and CHT's data. Put simply, the Filehne null-point is absent from their data. JJN therefore repeated the experiment, this time adjusting the dot velocity in the pursuit interval to match the perceived head-centred velocity in the eye-stationary interval. This ensures that speeds in the eye-stationary interval are presented in and around 0 (depending on the value randomly selected by the computer) and so forces the observer to reproduce matches close to the Filehne null-point. Despite this change, similar expansive transducers were required to fit these data.

In summary, Experiment 3 shows some observers produce substantially linear behaviour in general velocity-matching experiments whereas others do not. For those observers who display non-linear behaviour the type of non-linearity inferred from the transducer model is expansive. We find no evidence for general velocity-matching behaviour governed by compressive retinal and extra-retinal transducers, in agreement with Turano and Massof (2001).

8. General discussion

The visual system must compensate for the retinal motion created during an eye movement in order to estimate object motion and self-motion with respect to the head. The transducer model was identified as a straightforward account of this process. At its heart is the idea that perceived head-centred motion is the sum of two signals: a retinal signal coding motion on the retina and an extra-retinal signal coding motion of the eye. As pointed out, much previous work has concentrated on the degree to which the extra-retinal signal depends on the spatiotemporal structure of the image (Post & Leibowitz, 1985; Wertheim, 1987, 1994; Freeman & Banks,

1998). The question of the underlying shape of the speed transduction process has largely been ignored. The principle aim of this paper was to explore the impact of linear and non-linear speed transduction on perceived head-centred motion. Three instances of the transducer model were examined: linear, non-linear and hybrid. The linear model defined itself; the non-linear model did not because of the lack of guidance from the literature of relevant non-linear speed transducers to adopt. We chose to study speed transducers based on power laws. The hybrid model combined both linear and non-linear components.

The performance of these models was compared in three different situations: speed-matching (Aubert–Fleischl phenomenon), motion nulling (Filehne illusion) and general velocity matching. Two fundamental theoretical aspects of these models were identified. First, both models contain one free parameter when applied to speed-matching or motion nulling and, in the case of the linear model, general velocity matching. For the linear model the free parameter is the ratio of gains and for the non-linear model it is the ratio of powers. Second, the non-linear model produces general velocity-matching functions that depend uniquely on the absolute values of the powers. This implies that general velocity matching can in principle reveal the shapes of retinal and extra-retinal transducers, albeit up to an unknown scale factor.

The hybrid model was found to be unnecessarily complex, in that the additional parameters improved fits but only marginally so (and in the case of the general velocity matching experiments, not at all). We therefore concentrated on linear and non-linear models. In the case of the Aubert–Fleischl, the non-linear model provided the superior fit but the improvement was relatively minor given the 16-fold range of object speeds examined. In the case of the Filehne illusion, the linear model provided the superior fit, but again discriminating between the two models was difficult as the differences between them were small. This was not the case for general velocity matching. However, the results were variable in that some observers quite clearly showed non-linear behaviour whereas others showed approximately linear behaviour.

According to the transducer model, the type of non-linearities revealed by the general velocity-matching experiments were expansive for those observers exhibiting non-linear behaviour. No evidence was found for compressive speed transduction in any of our observers. A series of control experiments showed the expansive behaviour to be quite resistant to various manipulations such as shorter durations and change of method. For the remainder of the discussion we examine support for this surprising conclusion.

8.1. Magnitude estimation

The method of magnitude estimation could potentially yield the relationship between a physical dimension and its perceptual correlate (Georgeson, 1991). Kennedy, Yessenow, and Wendt (1972) found a linear relationship between the speed of a moving stimulus and magnitude estimates, in contrast to Rachlin (1966) who found compressive power functions. More recently, Kennedy, Hettinger, Harm, Ordy, and Dunlap (1996) found linear relationships for estimates of vection speed of observers placed inside a rotating drum. How far one is at liberty to interpret magnitude estimates as evidence for particular types of transducer is questionable. Nevertheless, as far as we are aware only one study has reported an expansive relationship between speed and magnitude estimate (Ekman & Dahlback, 1956) and this is in an obscure lab report cited by Rachlin (1966). At a qualitative level, therefore, the expansive behaviour exhibited by some observers does not gain much support from studies of speed magnitude estimation.

8.2. Heading perception

Neither does it gain much support from studies of heading perception during eye movements. The way in which speed is transduced is critical to extra-retinal accounts of eye-movement compensation when judging the direction of self-motion from retinal flow. The extra-retinal hypothesis predicts distortions in the perceived path because, as demonstrated by the Filehne illusion and Aubert–Fleischl phenomenon, retinal and extra-retinal motion signals are unequal. Path distortions have been reported for both constant (Freeman, 1999) and sinusoidal eye movements (the slalom illusion: Freeman et al., 2000). Importantly, the degree to which the distortion changes with pursuit speed depends on the transducers underlying the compensation process. Freeman (1999) showed that empirically-derived gain ratios remained approximately constant across a four-octave change in pursuit speed. This was true for slow and fast simulated translation speeds, as well as a Filehne condition in which the translation speed was zero. Experiments on heading perception therefore provide support for the linear model. Moreover, all three conditions in Freeman (1999) used a large ground-plane stimulus to carry the appropriate flow pattern. The findings of Experiment 2 therefore generalise to other stimuli (ground-planes) and to other judgements (self-motion).

8.3. Reference-signal models

What other explanations are there for the expansive non-linearity exhibited by some observers in general

velocity matching? Our data are in good agreement with the stabilised-viewing data of Turano and Massof (2001). The only possible discrepancy is the variability across observers found here. In our experiments we found considerable differences between individuals whereas little is seen Fig. 4 of Turano and Massof (2001). All their observers exhibited similar non-linear matching behaviour. The reason for the discrepancy may be in the different ranges of pursuit and retinal speeds investigated by the two studies, although it must also be pointed out that we are discussing only a handful of observers in each case. Turano and Massof rejected a class of non-linear transducers that compressed both retinal and extra-retinal speed. To model their data, however, they did not consider expansive transducers but instead proposed that perceived head-centred motion was based on the sum of a compressive retinal signal and a compressive compensation signal comprising both retinal and extra-retinal components. The latter, as they point out, is similar to the reference signal proposed by Wertheim (1994) because it comprises both retinal and extra-retinal components. Whether this type of model is a viable explanation of the data remains to be seen. Neither the transducer model nor the reference-signal model lead to very palatable conclusions. The first calls for expansive speed non-linearities to explain the general velocity-matching of some individuals. The second, as far we understand it, incorporates a somewhat odd redundancy because the same signal feeds both the retinal signal and the reference signal. Put another way, the reference-signal model includes a compensation signal that is compared to a retinal signal which is itself part of (or input to) the compensation signal.

8.4. Observer strategy and choice of reference frame

Is there another explanation for the non-linear behaviour displayed by some individuals? The settings in Experiment 3 tend to flatten out for head-centred velocities in the same direction as the pursuit. One interpretation of these data is that observers tend to ignore the velocity of the dots in favour of the velocity of the fixation point (or attached window), at least when dot velocity is close to that of the eye movement. How might such a strategy arise? All our observers were instructed to judge the head-centred motion of the dots but we have no way of telling if they obeyed these instructions or used some other reference frame to judge dot motion. For instance, one could attempt to judge the motion of the dots with respect to the fixation point by completely ignoring the fact the eyes are moving. This would be a retina-centred strategy. Another strategy, one that is quite clearly apparent when these stimuli are viewed, is to consider the dots as though they are sliding across the surface of an object (e.g. a conveyer belt) which is itself moving at the velocity of the fixation point and window. In this case, one could choose to ignore the head-centred motion of the dots and judge the motion of the underlying object. There is considerable evidence that the judgement of a target's motion depends on the reference frame chosen by the observer. For instance, the movement of larger backgrounds can give rise to apparent movement in stationary targets (Duncker, 1929; Wallach, 1959). They can also cause the apparent path of a moving object to deviate from the true path (Heckman, Post, & Deering, 1991) and determine the ability to detect speed changes in targets tracked by the eye (Brenner, 1991; Brenner & van den Berg, 1994, 1996). However, it is not clear how these findings relate to the current speculation because it is velocity of the 'background' random dot pattern that is being judged by our observers, not the velocity of the 'target' fixation point. Nevertheless, it remains possible that for some observers general velocity matching is contaminated by changes in strategy and not expansive speed transduction.

Acknowledgements

The author would like to thank Jenny Naji and Jane Sumnall for help in data collection; Marty Banks, Mike Landy, Mike Oaksford and Bob Snowden for helpful discussion; and two anonymous reviewers for their improvements to the manuscript. The work was supported by a project grant from the Wellcome Trust.

Appendix A

A.1. Linear model for general velocity matching

Perceived velocity of eye-stationary interval:

$$\hat{\mathbf{H}}_{es} = r\mathbf{H}_{es} \tag{A1}$$

Perceived velocity of pursuit interval is the sum of retinal and extra-retinal estimates of velocity:

$$\hat{\mathbf{H}}_{p} = e\mathbf{P} + r(\mathbf{H}_{p} - \mathbf{P}) \tag{A2}$$

(note $(\mathbf{H}_{p} - \mathbf{P})$ is the retinal velocity). At the match point, $\hat{\mathbf{H}}_{es} = \hat{\mathbf{H}}_{p}$. Using this expression and solving for $\mathbf{H}_{es}$:

$$\mathbf{H}_{es} = \mathbf{H}_{p} + \left(\frac{e}{r} - 1\right)\mathbf{P} \tag{A3}$$

The Filehne illusion sets $\mathbf{H}_{es}$ to 0, from which Eq. (5) in the main text follows.

A.2. Non-linear model for general velocity matching

From Eq. (3) with $a = 1$, perceived velocity of eye-stationary interval:

$$\hat{\mathbf{H}}_{es} = \mathrm{sgn}(\mathbf{H}_{es}) \times [(|\mathbf{H}_{es}| + 1)^{\rho}] - 1 \quad \text{(A4)}$$

Perceived velocity of pursuit interval is the sum of non-linear retinal and extra-retinal estimates of velocity:

$$\hat{\mathbf{H}}_{p} = \mathrm{sgn}(\mathbf{H}_{p} - \mathbf{P}) \times [(|\mathbf{H}_{p} - \mathbf{P}| + 1)^{\rho}] - 1 + \mathrm{sgn}(\mathbf{P}) \times [(|\mathbf{P}| + 1)^{\varepsilon}] - 1 \quad \text{(A5)}$$

where, as in Eq. (A2), $\mathbf{H}_{p} - \mathbf{P}$ is the retinal velocity. At the match point, $\hat{\mathbf{H}}_{es} = \hat{\mathbf{H}}_{p}$ which gives:

$$\mathrm{sgn}(\mathbf{H}_{es}) \times [(|\mathbf{H}_{es}| + 1)^{\rho}] = \mathrm{sgn}(\mathbf{H}_{p} - \mathbf{P}) \times [(|\mathbf{H}_{p} - \mathbf{P}| + 1)^{\rho}] + \mathrm{sgn}(\mathbf{P}) \times [(|\mathbf{P}| + 1)^{\varepsilon}] - 1 \quad \text{(A6)}$$

References

Abadi, R. V., Whittle, J. P., & Worfolk, R. (1999). Oscillopsia and tolerance to retinal image movement in congenital nystagmus. *Investigative Ophthalmology and Visual Science*, *40*, 339–345.

Aubert, H. (1886). Die Bewegungsempfindung. *Pflügers Archiv.*, *39*, 347–370.

Bahill, A. T., Iandolo, M. J., & Todd Troost, B. T. (1980). Smooth pursuit eye movements in response to unpredictable target waveforms. *Vision Research*, *20*, 923–931.

Bedell, H. E., & Currie, D. C. (1993). Extraretinal signals for congenital nystagmus. *Investigative Ophthalmology and Visual Science*, *34*, 2325–2332.

Beintema, J. A., & van den Berg, A. V. (1998). Heading detection using motion templates and eye velocity gain fields. *Vision Research*, *38*, 2155–2179.

Brenner, E. (1991). Judging object motion during smooth pursuit eye-movements—the role of optic flow. *Vision Research*, *31*, 1893–1902.

Brenner, E., & van den Berg, A. V. (1994). Judging object velocity during smooth-pursuit eye-movements. *Experimental Brain Research*, *99*, 316–324.

Brenner, E., & van den Berg, A. V. (1996). The special rule of distant structures in perceived object velocity. *Vision Research*, *36*, 3805–3814.

Collewijn, H., & Tamminga, E. P. (1984). Human smooth and saccadic eye-movements during voluntary pursuit of different target motions on different backgrounds. *Journal of Physiology, London*, *351*, 217–250.

de Graaf, B., & Wertheim, A. H. (1988). The perception of object motion during smooth pursuit eye-movements—adjacency is not a factor contributing to the Filehne illusion. *Vision Research*, *28*, 497–502.

Dichgans, J., & Brandt, T. (1972). Visual-vestibular interaction and motion perception. In J. Dichgans, & E. Bizzi, *Cerebral control of eye movements. Bibliotheca Opthalmologica*, vol. 82. Basel: Karger.

Dichgans, J., Wist, E., Diener, H. C., & Brandt, T. (1975). The Aubert–Fleischl phenomenon: a temporal frequency effect on perceived velocity in afferent motion perception. *Experimental Brain Research*, *23*, 529–533.

Duncker, K. (1929). Uber induzierte Bewegung. *Psychologische Forschung*, *12*, 180–259.

Ekman, G. & Dahlback, B. (1956). A subjective scale of velocity (31), Psychology Lab, University of Stockholm.

Filehne, W. (1922). Uber das optische Wahrnehmen von Bewegungen. *Zeitschrift für Sinnephysiologie*, *53*.

Fleischl, E. V. (1882). Physiologisch-optische Notizen, 2. Mitteilung. *Sitzung Wiener Bereich der Akademie der Wissenschaften*, *3*, 7–25.

Fotheringham, A. S., & Knudsen, D. C. (1987). *Goodness-of-fit statistics*. Norwich: Geo Books.

Freeman, T. C. A. (1999). Path perception and Filehne illusion compared: model and data. *Vision Research*, *39*, 2659–2667.

Freeman, T. C. A., & Banks, M. S. (1998). Perceived head-centric speed is affected by both extra-retinal and retinal errors. *Vision Research*, *38*, 941–945.

Freeman, T. C. A., Banks, M. S., & Crowell, J. A. (2000). Extraretinal and retinal amplitude and phase errors during Filehne illusion and path perception. *Perception and Psychophysics*, *62*, 900–909.

Georgeson, M. A. (1991). Over the limit: encoding contrast above threshold in human vision. In J. J. Kulikowski (Ed.), *Limits of visual perception*, vol. 5.

Haarmeier, T., & Thier, P. (1996). Modification of the Filehne illusion by conditioning visual stimuli. *Vision Research*, *36*, 741–750.

Heckman, T., Post, R. B., & Deering, L. (1991). Induced motion of a fixated target-influence of voluntary eye deviation. *Perception and Psychophysics*, *50*, 230–236.

Kennedy, R. S., Hettinger, L. J., Harm, D. L., Ordy, J. M., & Dunlap, W. P. (1996). Psychophysical scaling of circular vection (CV) produced by optokinetic (OKN) motion: Individual differences and effects of practice. *Journal of Vestibular Research-Equilibrium and Orientation*, *6*, 331–341.

Kennedy, R. S., Yessenow, M. D., & Wendt, G. R. (1972). Magnitude estimation of visual velocity. *Journal of Psychology*, *82*, 133–144.

Lappe, M., Bremmer, F., & van den Berg, A. V. (1999). Perception of self-motion from visual flow. *Trends in Cognitive Sciences*, *3*, 329–336.

Leigh, R. J., & Zee, D. S. (1999). *The neurology of eye movements*. Oxford: Oxford University Press.

Leigh, R. J., Dell'Osso, L. F., Yaniglos, S. S., & Thurston, S. E. (1988). Oscillopsia, retinal image stabilization and congenital nystagmus. *Investigative Ophthalmology and Visual Science*, *29*, 279–282.

Li, L., & Warren, W. H. (2000). Perception of heading during rotation: sufficiency of dense motion parallax and reference objects. *Vision Research*, *40*, 3873–3894.

Mack, A. & Herman, E. (1973). Position constancy during pursuit eye movement: an investigation of the Filehne illusion. *Quarterly Journal of Experimental Psychology, Experimental-Psychology*.

Mack, A., & Herman, E. (1978). The loss of position constancy during pursuit eye movements. *Vision Research*, *18*, 55–62.

Meyer, C. H., Lasker, A. G., & Robinson, D. A. (1985). The upper limit of human smooth pursuit velocity. *Vision Research*, *25*, 561–563.

Perrone, J. A., & Stone, L. S. (1994). A model of self-motion estimation within primate extrastriate visual-cortex. *Vision Research*, *34*, 2917–2938.

Post, R. B., & Leibowitz, H. W. (1985). A revised analysis of the role of efference in motion perception. *Perception*, *14*, 631–643.

Rachlin, H. C. (1966). Scaling subjective velocity, distance, and duration. *Perception and Psychophysics*, *1*, 77–82.

Raymond, J. E., Shapiro, K. L., & Rose, D. J. (1984). Optokinetic backgrounds affect perceived velocity during ocular tracking. *Perception and Psychophysics*, *36*, 221–224.

Royden, C. S., Banks, M. S., & Crowell, J. A. (1992). The perception of heading during eye-movements. *Nature*, *360*, 583–587.

Royden, C. S., Crowell, J. A., & Banks, M. S. (1994). Estimating heading during eye-movements. *Vision Research*, *34*, 3197–3214.

Smith, A. T., & Edgar, G. K. (1991). The influence of spatial-frequency on perceived temporal frequency and perceived speed. *Vision Research*, *30*, 1467–1474.

Stone, L. S., & Thompson, P. (1992). Human speed perception is contrast dependent. *Vision Research*, *32*, 1535–1549.

Treue, S., Snowden, R., & Andersen, R. A. (1993). The effect of transiency on perceived velocity of visual patterns: a case of 'temporal capture'. *Vision Research*, *33*, 791–798.

Turano, K. A., & Massof, R. W. (2001). Nonlinear contribution of eye velocity to motion perception. *Vision Research*, *41*, 385–395.

van den Berg, A. V. (1992). Robustness of perception of heading from optic flow. *Vision Research*, *32*, 1285–1296.

van den Berg, A. V. (1996). Judgements of heading. *Vision Research*, *36*, 2337–2350.

Wallach, H. (1959). The perception of motion. *Scientific American*, *201*, 56–60.

Wertheim, A. H. (1987). Retinal and extraretinal information in movement perception—how to invert the Filehne illusion. *Perception*, *16*, 299–308.

Wertheim, A. H. (1994). Motion perception during self-motion—the direct versus inferential controversy revisited. *Behavioral and Brain Sciences*, *17*, 293–311.

Yee, R. D., Daniels, S. A., Jones, O. W., Baloh, R. W., & Honrubia, V. (1983). Effects of an optokinetic background on pursuit eye-movements. *Investigative Ophthalmology and Visual Science*, *24*, 1115–1122.